Journal of Molecular Cell Biology (2023), 15(5), mjad035 https://doi.org/10.1093/jmcb/mjad035
Published online May 27, 2023

Article

Human umbilical cord-derived mesenchymal stem cells alleviate oxidative stress-induced islet impairment via the Nrf2/HO-1 axis

Peng Liu[1,†], Baige Cao[2,†], Yang Zhou[3], Huina Zhang[4], and Congrong Wang[2,*]

[1] Shanghai Diabetes Institute, Department of Endocrinology and Metabolism, Shanghai Key Laboratory of Diabetes Mellitus, Shanghai Sixth People's Hospital Affiliated to Shanghai Jiao Tong University School of Medicine, Shanghai 200233, China
[2] Department of Endocrinology & Metabolism, Shanghai Fourth People's Hospital, School of Medicine, Tongji University, Shanghai 200434, China
[3] Translational Medical Center for Stem Cell Therapy, Shanghai East Hospital, School of Medicine, Tongji University, Shanghai 200092, China
[4] Stem Cell Translational Research Center, Tongji Hospital, School of Medicine, Tongji University, Shanghai 200065, China
[†] These authors contributed equally to this work.
[*] Correspondence to: Congrong Wang, E-mail: crwang@tongji.edu.cn

Edited by Feng Liu

Hyperglycaemia-induced oxidative stress may disrupt insulin secretion and β-cell survival in diabetes mellitus by overproducing reactive oxygen species. Human umbilical cord-derived mesenchymal stem cells (hUC-MSCs) exhibit antioxidant properties. However, the mechanisms by which hUC-MSCs protect β-cells from high glucose-induced oxidative stress remain underexplored. In this study, we showed that intravenously injected hUC-MSCs engrafted into the injured pancreas and promoted pancreatic β-cell function in a mouse model of type 1 diabetes mellitus. The *in vitro* study revealed that hUC-MSCs attenuated high glucose-induced oxidative stress and prevented β-cell impairment via the Nrf2/HO-1 signalling pathway. Nrf2 knockdown partially blocked the anti-oxidative effect of hUC-MSCs, resulting in β-cell decompensation in a high-glucose environment. Overall, these findings provide novel insights into how hUC-MSCs protect β-cells from high glucose-induced oxidative stress.

Keywords: type 1 diabetes, β-cell protection, mesenchymal stem cells, oxidative stress, Nrf2

Introduction

Type 1 diabetes mellitus (T1DM) is an autoimmune disease characterized by impaired pancreatic β-cells, resulting in absolute insulin deficiency. Despite significant efforts in diabetes management, glycaemic control remains non-optimized. Most people with T1DM continuously have the degenerating insulin-producing β-cells, unless on-going glucotoxicity and autoimmune destruction of β-cells are inhibited (Meier et al., 2005). Although insulin independence can now be achieved by whole-pancreas or isolated islet transplantation (Aguayo-Mazzucato, 2010), the insufficient supply of donor islets and the difficulty in controlling immune rejection limit the number of patients who can benefit from islet transplantation (Pellegrini et al., 2018).

In recent years, mesenchymal stem cells (MSCs) have emerged as a new and potential source of regenerative therapies for DM. MSCs are a population of stromal cells that can self-renew, migrate, perform paracrine functions, and have pluripotency. MSCs were isolated from various sources, such as adipose tissue, bone marrow, and umbilical cord, have been studied for treating DM (Gao et al., 2014; Rahavi et al., 2015; Maldonado et al., 2017). Human umbilical cord-derived MSCs (hUC-MSCs) are isolated from extra-embryonic tissues. Owing to their tissue regenerative properties and immunomodulatory effects, hUC-MSCs may be more promising than the MSCs derived from the adipose tissue and bone marrow in the clinical studies (Alunno et al., 2015). hUC-MSCs exert potential therapeutic effects in a streptozotocin (STZ)-induced animal model. An intravenous infusion of hUC-MSCs prevented hyperglycaemic progression and preserved islet size and number in STZ-induced diabetic rats (Zhou et al., 2015), and an intraperitoneal injection of hUC-MSCs promoted insulin secretion from pancreatic islets (Maldonado et al., 2017). However, whether intraperitoneally injected MSCs can migrate into the damaged

Received May 11, 2022. Revised January 10, 2023. Accepted February 14, 2023.

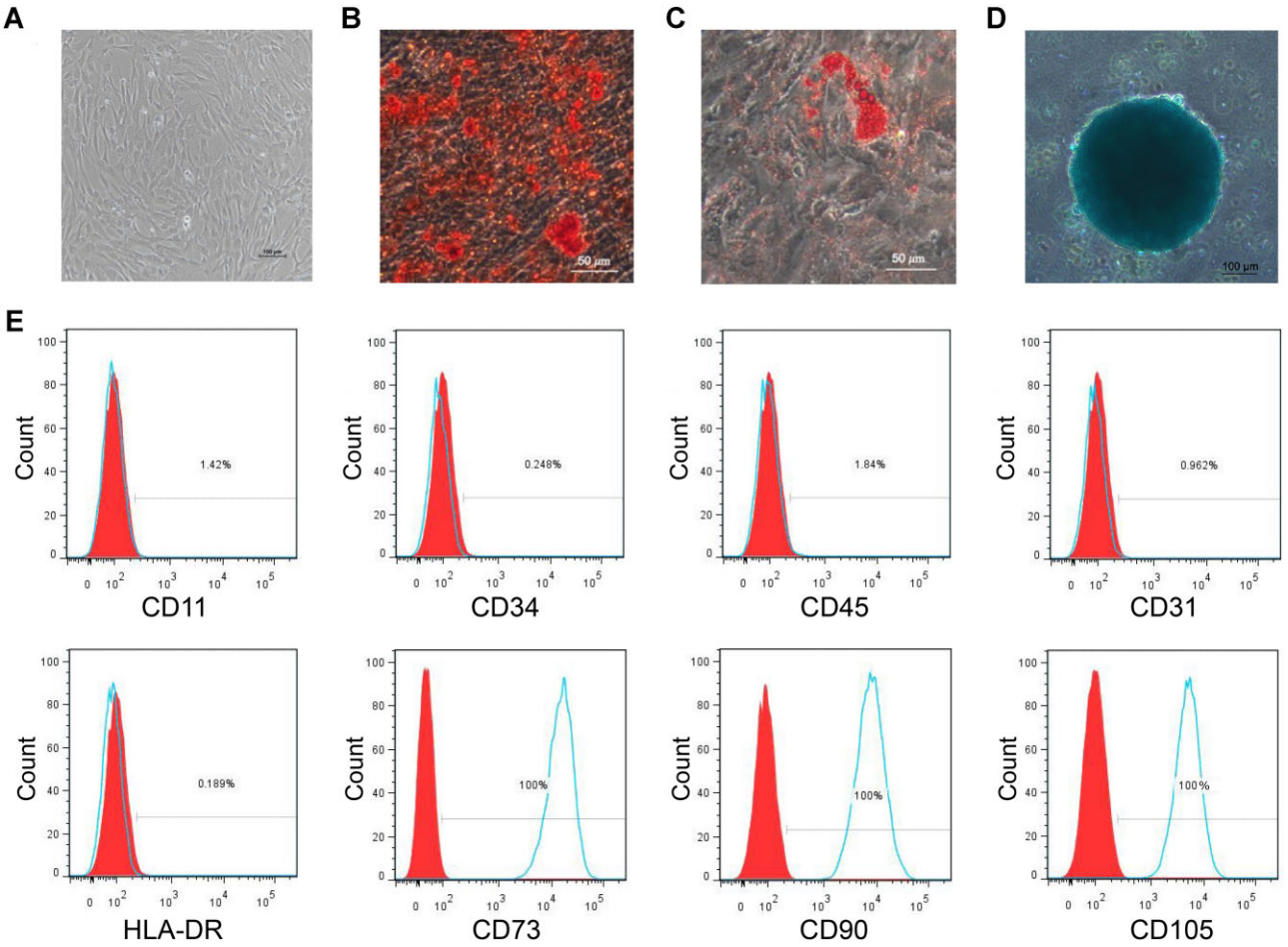

Figure 1 Morphology and characterization of hUC-MSCs. (**A**) Morphology of hUC-MSCs. Scale bar, 100 μm. (**B**–**D**) Three-lineage differentiation of hUC-MSCs. (**B**) hUC-MSCs differentiated into osteocytes, indicated by alkaline phosphatase staining with alizarin red S. Scale bar, 50 μm. (**C**) hUC-MSCs differentiated into adipocytes, indicated by the formation of lipid vesicles stained with oil red O. Scale bar, 50 μm. (**D**) hUC-MSCs differentiated into chondrocytes, stained with alcian blue. Scale bar, 100 μm. (**E**) Specific cell surface markers were assessed by fluorescence-activated cell sorting. hUC-MSCs were positive for CD73, CD90, and CD105 but negative for CD11, CD34, CD45, CD31, and HLA-DR.

pancreas and the mechanisms underlying these therapeutic effects are unclear.

Chronic hyperglycaemia has been linked to overproduced cellular levels of reactive oxygen species (ROS). Hyperglycaemia-induced ROS generation causes pancreatic β-cell apoptosis (Kim et al., 2007). Meanwhile, the endogenous antioxidant defence system comprising several antioxidant enzymes, such as superoxide dismutase, catalase, glutathione peroxidase, and heme oxygenase-1 (HO-1), counteracts high levels of ROS (Matés, 2000). Increasing evidence has shown that MSCs can restore oxidative balance and decrease tissue injury by releasing antioxidants (Shalaby et al., 2014; Liu et al., 2019). MSCs were reported to suppress ROS production in renal proximal tubular epithelial cells (Cao et al., 2020). Hence, we speculate that hUC-MSCs could play a protective role by inhibiting ROS production in pancreatic β-cells. Nuclear factor erythroid 2-related factor 2 (Nrf2), a key transcription factor, regulates the expression of genes involved in antioxidant response and cell survival (Uruno et al., 2015). Notably, adaptive Nrf2 activation could protect cells from ROS damage under oxidative stress (Shaw and Chattopadhyay, 2020). Interestingly, *in vivo* studies have shown that bone marrow-derived MSCs (BM-MSCs) or MSC-derived exosomes can alleviate brain or acute kidney injury via the Nrf2–ARE signalling pathway (Zhang et al., 2016; Chen et al., 2020). Given this scenario, further research into the protective effects of hUC-MSCs on oxidative stress-induced islet impairment and the underlying molecular mechanism is needed.

In the present study, STZ-induced diabetic mice were used to evaluate the *in vivo* therapeutic effects of clinical-grade hUC-MSCs via intravenous administration. We found that hUC-MSCs engrafted into the pancrease, ameliorated hyperglycaemia, and preserved β-cell function in STZ-induced diabetic mice. Further *in vitro* experiments indicated that hUC-MSCs could protect co-cultured INS-1E cells against high

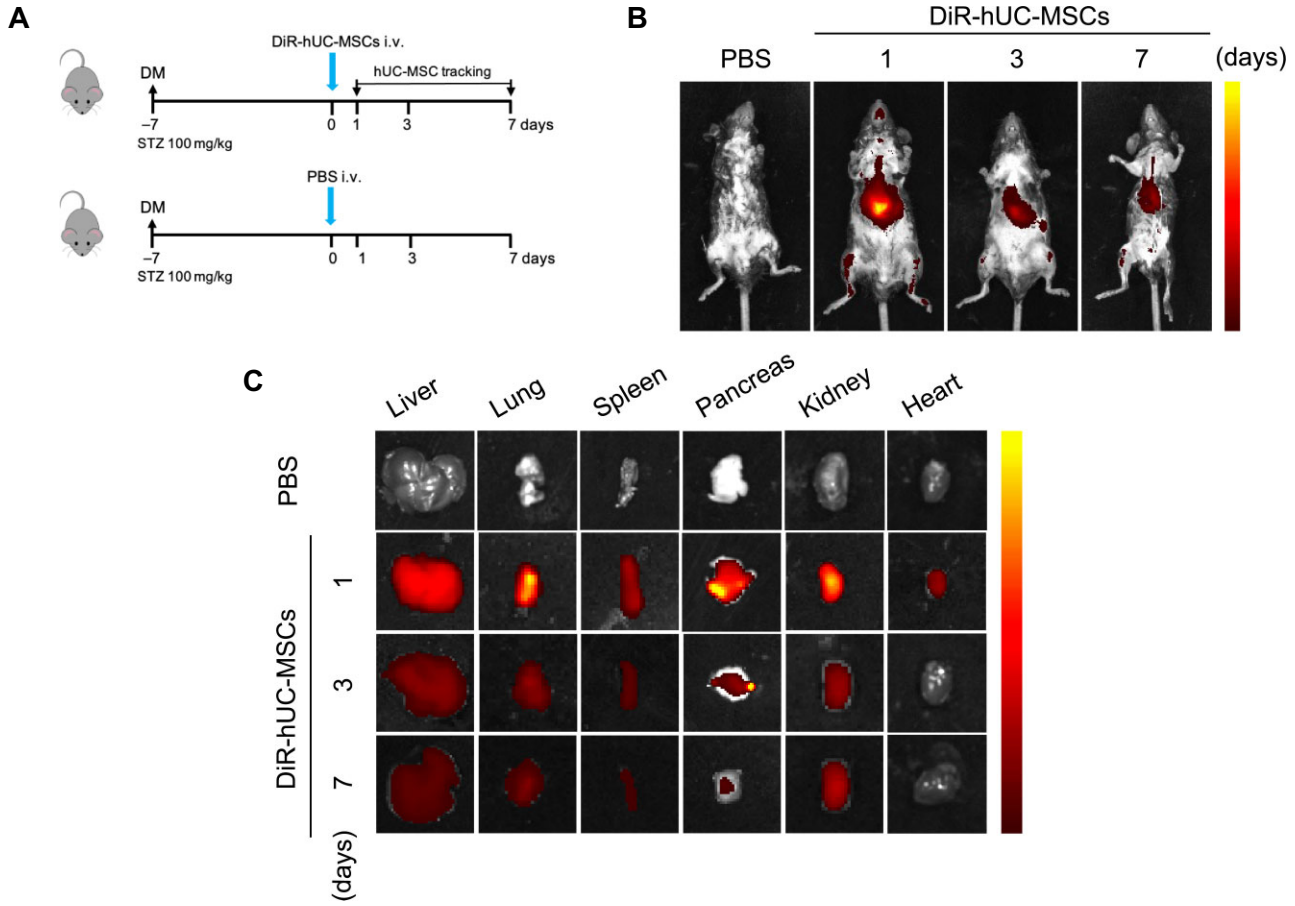

Figure 2 Bio-distribution of DiR-labelled hUC-MSCs in STZ-induced diabetic mice. (**A**) Study design for tracing hUC-MSC bio-distribution. Diabetic mice were administered DiR-labelled hUC-MSCs and imaged using the IVIS system or sacrificed at 1, 3, and 7 days after the infusion. Diabetic mice treated with PBS served as controls. i.v., intravenous injection. (**B**) Representative *in vivo* fluorescence images of hUC-MSCs labelled with DiR. (**C**) Representative *ex vivo* fluorescence images of hUC-MSCs labelled with DiR in mouse organs, including the liver, lung, spleen, pancreas, kidney, and heart.

glucose-induced cell apoptosis and improve glucose-stimulated insulin secretion (GSIS) by ameliorating oxidative damage and improving β-cell function via the Nrf2/HO-1 pathway. Thus, hUC-MSC transplantation could be a potential strategy for diabetes treatment through activating Nrf2 signalling.

Results

Characterization of hUC-MSCs

Our data showed that hUC-MSCs cultured to passage 4 exhibited a spindle-shaped morphology and plastic-adherent characteristics (Figure 1A). These cells could differentiate into osteoblasts, adipocytes, and chondrocytes under certain conditions (Figure 1B–D). Flow cytometry analyses revealed that hUC-MSCs were positive for CD73, CD90, and CD105 but negative for CD11, CD34, CD45, CD31, and HLA-DR (Figure 1E), demonstrating the stemness of the cultured cells.

Bio-distribution of hUC-MSCs

The diabetic mouse model was established by intraperitoneal injection of 100 mg/kg STZ and validated by measuring blood glucose levels and performing intraperitoneal glucose tolerance tests (IPGTTs). The STZ-administered group showed significantly higher blood glucose levels compared to the control group (Supplementary Figure S1A). Mice with >3 times of random blood glucose level $\geq$16.7 mmol/L were defined as diabetic mice. On Day 7 after STZ injection, the deterioration of glucose tolerance was observed (Supplementary Figure S1B). To assess the hUC-MSC bio-distribution, the diabetic mice were administered DiR-labelled hUC-MSCs and imaged at the indicated time points using an *in vivo* imaging system IVIS (Figure 2A). The fluorescence was detected at 24 h after administration and tapered gradually throughout 7 days in the DiR-hUC-MSC-treated group (Figure 2B). To assess the organ localization of hUC-MSCs, the diabetic mice were sacrificed at the indicated time points

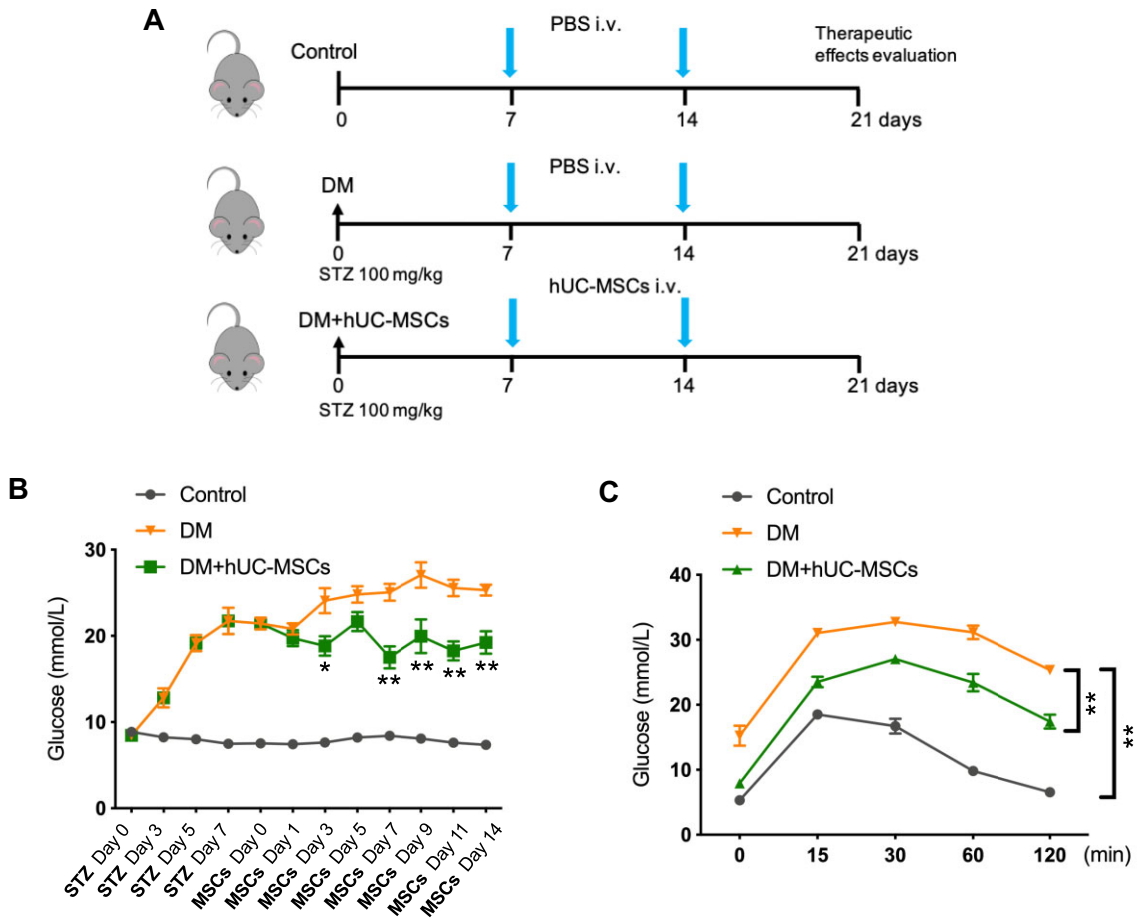

Figure 3 hUC-MSC administration improves glucose homeostasis in STZ-induced diabetic mice. (**A**) Study design for hUC-MSC therapies in diabetic mice. STZ-induced diabetic mice were randomly divided into the hUC-MSC-treated group (DM+hUC-MSCs) and the PBS-treated group (DM). Mice without STZ injection served as the control group. i.v., intravenous injection. (**B**) Random blood glucose levels were improved after hUC-MSC transplantation compared with that in the DM group. (**C**) One week after the second hUC-MSC infusion, glucose tolerance was improved after hUC-MSC transplantation compared with that in the DM group. The results are presented as mean ± SEM. $n = 6$ per group. $^{*}P < 0.05$, $^{**}P < 0.01$.

after DiR-hUC-MSC administration, and the pancreas, liver, lung, spleen, kidney, and heart were harvested and imaged *ex vivo*. Most hUC-MSCs accumulated in the liver, lung, pancreas, and kidney at 24 h after hUC-MSC injection. The signals for the liver, lung, spleen, pancreas, and kidney persisted for up to 7 days, while no positive signal was found in the heart after 3 days (Figure 2C).

hUC-MSC treatment improves glucose homeostasis and restores islet function in STZ-induced diabetic mice

The established diabetic mice (referred to as DM) were randomly treated with 0.2 ml phosphate-buffered saline (PBS) or 1×10^6 hUC-MSCs in 0.2 ml PBS through the tail vein once a week for 2 weeks. Normal mice treated with PBS served as controls (Figure 3A). The hyperglycaemia was ameliorated in hUC-MSC-treated DM group (Figure 3B and C).

Given the essential role of pancreatic β-cells in blood glucose regulation, islet function was examined. As shown in Figure 4A–C, the numbers of islets and insulin-producing cells were significantly reduced in the DM group compared with the control group. After hUC-MSC transplantation, both the size and number of pancreatic islets were restored, and the ratio of insulin-producing β-cells per islet was recovered (Figure 4A–C). In addition, the expression level of PDX-1 was significantly decreased in the DM group but recovered in the hUC-MSC-treated DM group (Figure 4D and E). GLUT2 membrane localization was significantly reduced in the DM group but restored by hUC-MSC treatment (Figure 4F and G). Moreover, treatment with hUC-MSCs improved the impaired GSIS in diabetic mice, evidenced by enzyme-linked immunosorbent assay (ELISA) (Figure 4H). Collectively, these findings showed that hUC-MSCs preserved islet morphologies, PDX-1 and GLUT2 expression levels, and GSIS, and thus improved islet function.

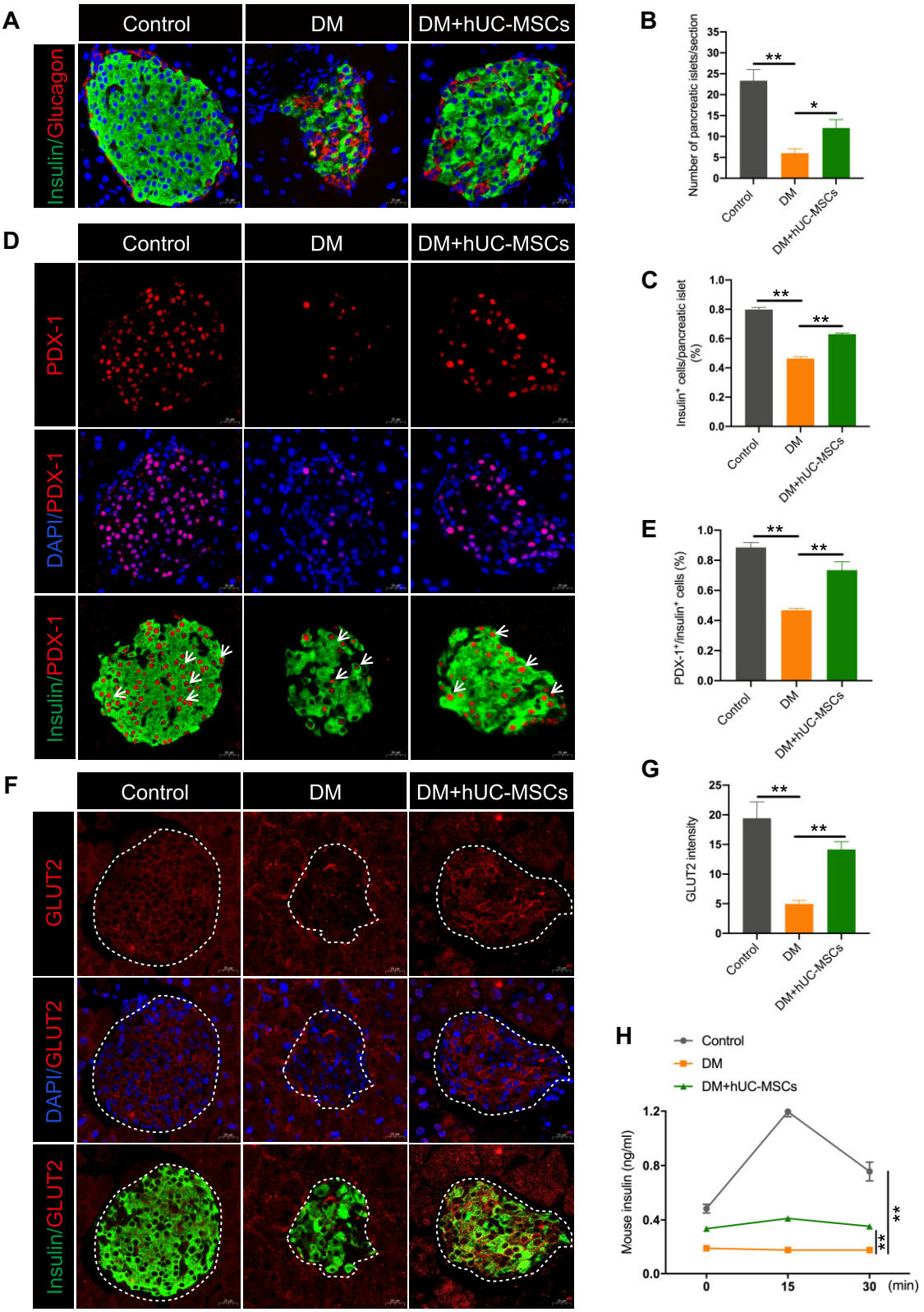

Figure 4 Administration of hUC-MSCs improves pancreatic islet function in STZ-induced diabetic mice. (**A**) Representative images of the immunolocalization of insulin (green), glucagon (red), and DAPI (blue) in mouse pancreatic tissues. (**B**) The number of pancreatic islets per section was increased in the DM+hUC-MSCs group compared with that in the DM group ($n = 6$ per group). (**C**) The percentage of insulin-producing cells in the pancreatic islet was improved in the DM+hUC-MSCs group compared to that in the DM group ($n = 6$ per group).

hUC-MSC treatment enhances insulin secretion, cell viability, and β-cell function and attenuates β-cell injury

To evaluate the effects of hUC-MSCs on β-cells, INS-1E cells were co-cultured with hUC-MSCs for 24 h in a Transwell device (Figure 5A). Since high glucose has been demonstrated to be toxic and deleterious to cultured β-cells, we evaluated whether hUC-MSCs could protect INS-1E cells against high glucose-induced injury. High glucose (30 mM) inhibited INS-1E cell viability compared with a normal glucose concentration (11.1 mM), which was reversed by hUC-MSC treatment (Figure 5B). To assess cell apoptosis, Annexin V-FITC and PI double staining was performed. The results showed that INS-1E cells exposed to high glucose had an increased apoptotic rate, which was significantly reduced by hUC-MSCs (Figure 5C).

Furthermore, high glucose inhibited GSIS in INS-1E cells, which was alleviated by co-culturing INS-1E cells with hUC-MSCs (Figure 5D). Western blotting revealed that the protein levels of GLUT2, PDX-1, MafA, and BCL-2 were significantly decreased whereas that of cleaved Caspase-3 was significantly increased in INS-1E cells exposed to high glucose, but all returned to normal when INS-1E cells were co-cultured with hUC-MSCs (Figure 5E). Consistently, in the pancreas of diabetic mice, hUC-MSC transplantation increased the protein levels of PDX-1, GLUT2, MafA, and BCL-2 but decreased that of cleaved Caspase-3 (Figure 5F).

hUC-MSCs inhibits oxidative stress and ROS formation in β-cells in response to high glucose in vitro

Oxidative stress leads to necrosis, apoptosis, inflammation, and other disorders. Growing evidence has shown that hyperglycaemia is responsible for the oxidative stress observed in the pancreatic β-cells in diabetic mice. To assess the anti-oxidative effects of hUC-MSCs on islets, ROS production in high glucose-treated INS-1E cells was examined by flow cytometry. Our data showed significantly increased ROS levels in high glucose-treated INS-1E cells, which were significantly reduced when INS-1E cells were co-cultured with hUC-MSCs (Figure 6A), suggesting that hUC-MSCs could protect β-cells against oxidative stress by blocking intracellular ROS production.

Nrf2 is a master transcriptional factor that mediates the intracellular defence mechanism by regulating the expression of antioxidant enzymes. HO-1, a cytoprotective effector of Nrf2, protects cells from oxidative injury while inhibiting apoptosis. To determine whether the Nrf2/HO-1 axis is involved in the anti-oxidative effects of hUC-MSCs, we examined the expression levels of Nrf2 and HO-1 in INS-1E cells. The results showed that hUC-MSCs significantly increased the mRNA and protein expression levels of both Nrf2 and HO-1 in high glucose-treated INS-1E cells (Figure 6B and C). Interestingly, *ex vivo* experiments also confirmed that hUC-MSC treatment enhanced the protein levels of Nrf2 and HO-1 in the pancreas of diabetic mice (Figure 6D).

Nrf2 knockdown blocks the anti-oxidative effects and β-cell function restoration by hUC-MSCs under high-glucose conditions

Next, we investigated whether hUC-MSCs contributed to the oxidant–antioxidant balance through Nrf2 signalling in INS-1E cells (Figure 7A) . Upon Nrf2 knockdown by small interfering RNA (siRNA), both protein and mRNA levels of Nrf2 and HO-1 were greatly reduced in INS-1E cells (Figure 7B).

Flow cytometry revealed that hUC-MSCs ameliorated high glucose-induced apoptosis and ROS production in INS-1E cells but failed to do so in cells transfected with Nrf2 siRNA (Figure 7C and D). Consistently, GSIS prompted by hUC-MSCs was suppressed after Nrf2 knockdown (Figure 7E).

Western blotting revealed that the enhanced protein levels of Nrf2 and HO-1 in INS-1E cells co-cultured with hUC-MSCs were reduced by Nrf2 siRNA transfection (Figure 7F). In addition, the upregulated expression levels of PDX-1, GLUT2, MafA, and BCL-2 were significantly decreased by Nrf2 knockdown, whereas the downregulated expression level of cleaved Caspase-3 was promoted (Figure 7G). Overall, these results demonstrated that Nrf2 knockdown partially blocked the anti-oxidative effects and β-cell function restoration by hUC-MSCs, indicating that Nrf2 may be involved in hUC-MSC-mediated β-cell protection against oxidative stress-induced islet impairment in diabetes.

Discussion

T1DM has been linked to the progressive loss of pancreatic β-cells (Katsarou et al., 2017). Previous studies indicated that hUC-MSCs could be an alternative source of stem cell therapy in treating diabetes due to their regenerative, anti-inflammatory, and immunomodulatory properties (Aguayo-Mazzucato, 2010; Zhou et al., 2015). A clinical trial showed that MSC-treated T1DM patients exhibited increased C-peptide levels during a mixed-meal tolerance test, suggesting that MSCs can preserve residual β-cell function (Carlsson et al., 2015). However, the mechanism underlying the therapeutic effects of MSCs remains unclear. In this study, we found that multiple intravenous infusions of hUC-MSCs reduced blood glucose levels and restored β-cell function in STZ-induced diabetic

Figure 4 *(Continued)* (**D**) Representative images of islets stained for insulin (green), PDX-1 (red), and DAPI (blue). The white arrows indicate PDX-1$^+$/insulin$^+$ cells. (**E**) The percentage of insulin-producing cells co-expressing PDX-1 was upregulated in the DM+hUC-MSCs group compared with that in the DM group ($n = 4$ per group). (**F**) Representative images of islets stained for insulin (green), GLUT2 (red), and DAPI (blue). The white dotted line circles pancreatic islets. (**G**) The integrated signal intensity of GLUT2 increased in the DM+hUC-MSCs group compared with that in the DM group ($n = 4$ per group). (**H**) Serum insulin was measured at 0, 15, and 30 min after glucose injection. The insulin secretion capacity was improved in the DM+hUC-MSCs group compared with that in the DM group ($n = 4$ per group). Scale bar, 20 μm. The results are presented as mean ± SEM. *$P < 0.05$, **$P < 0.01$.

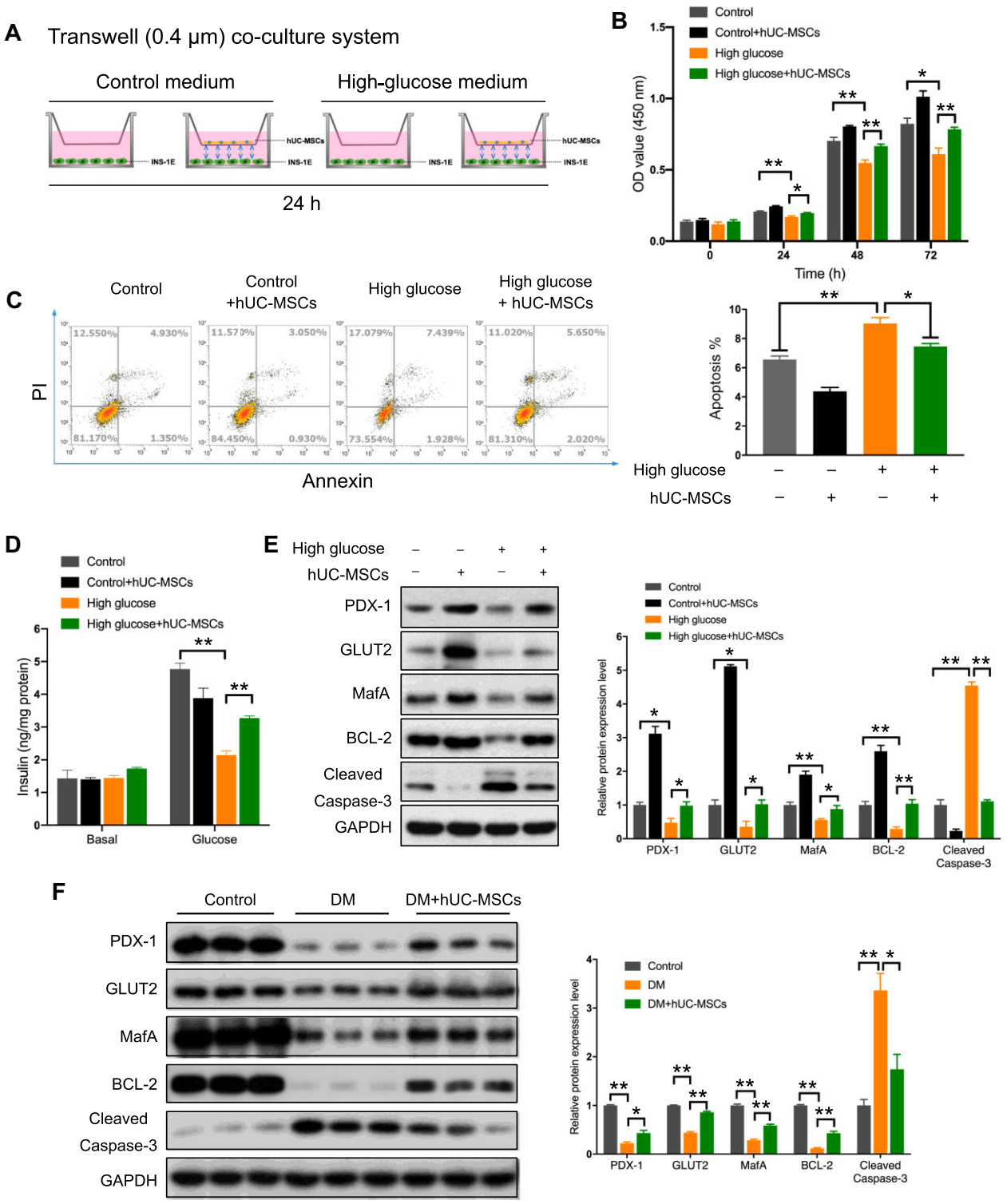

Figure 5 hUC-MSC treatment enhances cell viability, insulin secretion, and β-cell function and attenuates β-cell injury. (**A**) INS-1E cells were seeded into Transwell 6-well plates and incubated with or without hUC-MSCs for 24 h. Cells were exposed to high-glucose (30 mM) medium or normal medium. (**B**) The CCK-8 assay showing that high glucose-reduced cell growth rate of INS-1E cells was increased by hUC-MSCs. (**C**) Flow cytometry showing that glucose-induced INS-1E cell apoptosis was alleviated by hUC-MSCs. (**D**) GSIS was measured at 1 h after glucose stimulation (16.7 mM). ELISA showing that high glucose-reduced insulin concentration in INS-1E cell supernatant was increased by hUC-MSCs. (**E** and **F**) PDX-1, GLUT2, MafA, BCL-2, and cleaved Caspase-3 protein levels in INS-1E cells (**E**) and mouse pancreas tissues (**F**) were determined by western blotting. Protein expression levels were normalized to GAPDH. Data are presented as mean ± SEM. $^{*}P < 0.05$, $^{**}P < 0.01$.

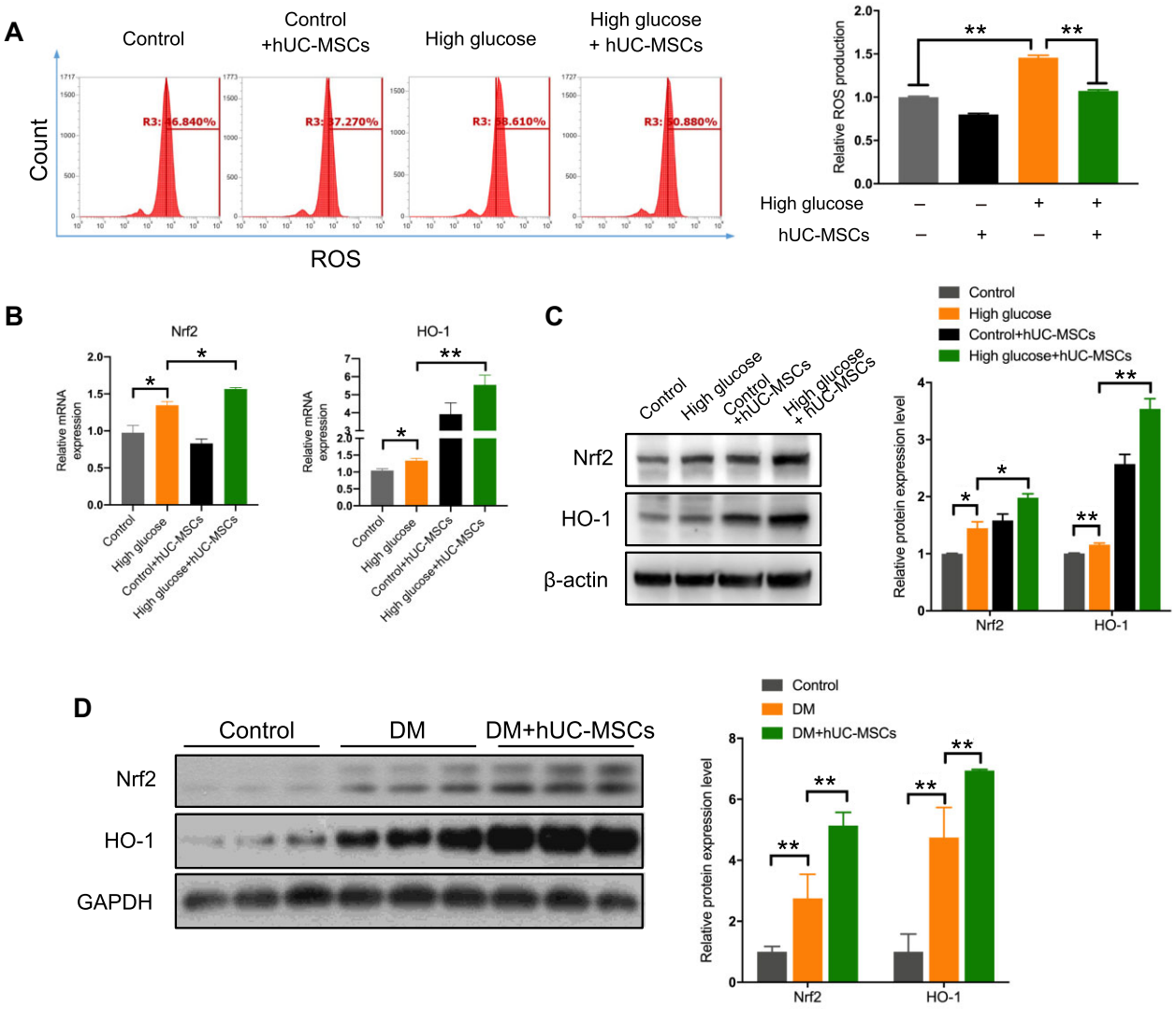

Figure 6 hUC-MSCs alleviate ROS levels in INS-1E cells via the Nrf2/HO-1 pathway under high-glucose conditions. (**A**–**C**) INS-1E cells cultured with or without hUC-MSCs were exposed to high-glucose (30 mM) medium or normal medium for 24 h. (**A**) Intracellular ROS were assessed by flow cytometry. hUC-MSCs significantly alleviated ROS in INS-1E cells upon high glucose. (**B**) mRNA expression levels of Nrf2 and HO-1. (**C**) Protein expression levels of Nrf2 and HO-1. Protein expression levels were normalized to β-actin. (**D**) hUC-MSC treatment enhanced Nrf2 and HO-1 protein levels in the pancreas of diabetic mice. Protein expression levels were normalized to GAPDH. Data are presented as mean ± SEM. *$P < 0.05$, **$P < 0.01$.

mice. We further demonstrated that the improved glucose homeostasis in hUC-MSC-treated diabetic mice was related to the Nrf2/HO-1 pathway activation. These findings suggest that hUC-MSCs could be used to treat patients with diabetes.

Several traditional methods for tracing the migration of transplanted donor cells in animal studies have been developed (Yin et al., 2018; Ullah et al., 2019). Previous studies showed that the intravenously transplanted Dil-labelled MSCs were mainly enriched in the liver, spleen, and lung of diabetic mice (Yin et al., 2018). In this study, we used non-invasive, *in vivo* imaging of MSCs to study cell movement and distribution in diabetic mice. We observed maximal fluorescence intensity from the whole body at 24 h after injection. The signal was clearly detectable throughout 7 days after cell transplantation and began to decay on Day 3. Further examination of the isolated organs (*ex vivo*) revealed a strong fluorescent signal in the liver, lung, and spleen, reflecting cell accumulation in blood vessel-rich tissues, consistent with previous reports (Yin et al., 2018). A weak signal was detected in the pancreas at 24 h post-injection and persisted for up to 7 days. Our results demonstrate that the transplanted hUC-MSCs engrafted into the injured pancreas, and bioluminescence imaging provides vital clues about the fate of transplanted MSCs *in vivo*.

Previous studies indicated that BM-MSCs could protect pancreatic β-cells from chronic high glucose-induced dysfunction by enhancing the autophagic activity or Wnt4–β-catenin signalling

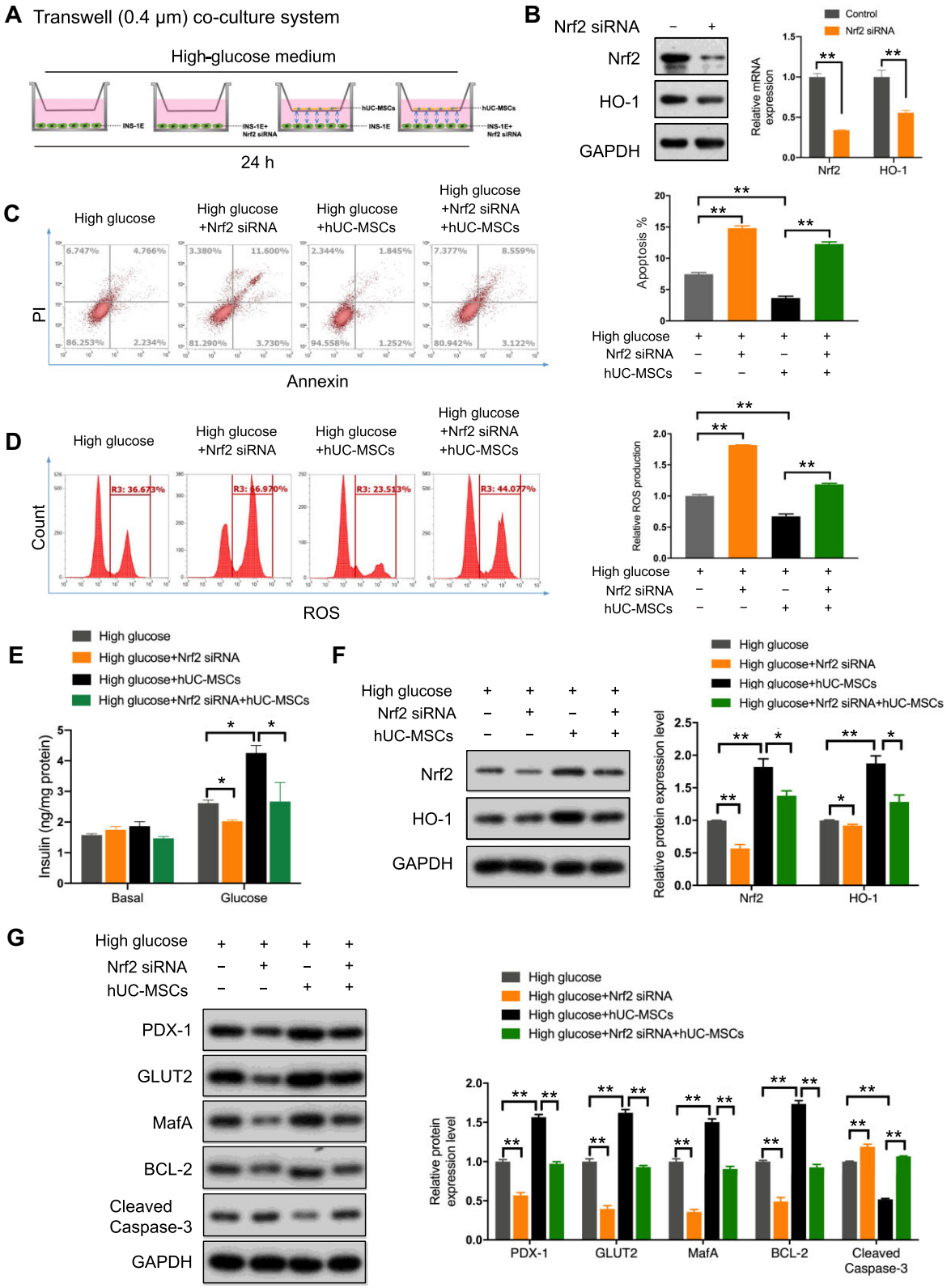

Figure 7 Nrf2 knockdown blocks the anti-oxidative effects and β-cell function restoration by hUC-MSCs under high-glucose conditions. (**A**) INS-1E cells were seeded into Transwell 6-well plates and treated with scrambled or Nrf2 siRNA. Then, INS-1E cells cultured with or without hUC-MSCs were exposed to high-glucose (30 mM) medium or normal medium for 24 h. (**B**) Nrf2 siRNA knockdown was confirmed by western blotting and quantitative real-time PCR. (**C**) Apoptosis of INS-1E cells was analysed by flow cytometry.

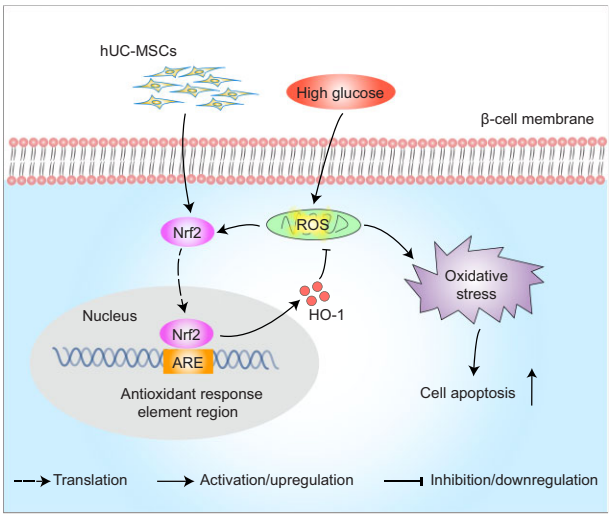

Figure 8 Schematic diagram showing that hUC-MSCs protect pancreatic β-cells against high glucose-induced oxidative stress via the Nrf2/HO-1 signalling pathway.

(Zhao et al., 2015; Wang et al., 2017). In addition, human adipose tissue-derived MSCs (hAD-MSCs) from non-diabetic donors improved hyperglycaemia and preserved pancreatic β-cell mass in STZ-induced mice. Notably, tissue inhibitor of metalloproteinase 1 secreted by hAD-MSCs was identified as a novel factor responsible for the pro-survival effects under pro-inflammatory conditions (Kono et al., 2014). However, MSCs harvested from different tissue sources might exhibit different therapeutic characteristics. When the therapeutic properties of hAD-MSCs and hUC-MSCs for T2DM were compared under the same experimental conditions, hUC-MSCs were more effective than hAD-MSCs in improving hyperglycaemia, insulin resistance, and dyslipidaemia in mice with T2DM (Ma et al., 2021). Owing to the therapeutic potential and ease of access via non-invasive procedures, hUC-MSCs have received more attention for DM treatment in recent years.

Administration routes are critical for stem cell therapies. Intraperitoneal and pancreatic artery injections were used in previous studies (Hu et al., 2013; Cai et al., 2016; Maldonado et al., 2017). Intravenous infusion is a popular route for MSC transplantation owing to its safety and less rigorous technical requirements (Chrostek et al., 2019). Intravenous injections of AD-MSCs exhibited beneficial effects on the T1DM mouse model (Lv et al., 2020). In addition, BM-MSC transplantation can ameliorate hyperglycaemia and improve β-cell function in diabetic mice (Gao et al., 2014; Yaochite et al., 2016). Unlike BM-MSCs or AD-MSCs, hUC-MSC isolation is a less invasive procedure. In this study, we found that systemic administration of hUC-MSCs to STZ-induced diabetic mice resulted in a gradual decrease in blood glucose levels until the end of the study, together with the recovery of pancreatic β-cells. β-cells are highly sensitive to glucose, consistently secreting corresponding amounts of insulin in response to increasing glucose concentrations. *In vitro*, we also observed that under high-glucose conditions, INS-1E cells co-cultured with hUC-MSCs exhibited higher cell viability, lower ROS production, and higher insulin secretion than the control group, corroborating the *in vivo* study in STZ-induced diabetic mice. Therefore, hUC-MSCs may promote islet β-cell restoration.

Reportedly, oxidative stress plays a crucial role in the pathogenesis of diabetes, which is mainly triggered by glucotoxicity. Patients with diabetes have high levels of oxidative stress (Zhang et al., 2020). Persistent oxidative stress eventually leads to glucose-induced β-cell apoptosis (Lu et al., 2011). Therefore, glucose-induced oxidative stress may be a potential therapeutic target for diabetes. A previous study showed that MSC treatment repaired oxidative stress-induced skin injury in mice and alleviated cellular responses to oxidative stress (Motegi et al., 2017). Notably, our study showed that hUC-MSC treatment alleviated ROS generation and apoptosis whereas elevated antioxidant enzyme levels in INS-1E cells under high-glucose conditions.

Pancreatic β-cells are extremely vulnerable to oxidative stress due to low expression levels of antioxidant enzymes (Tiedge et al., 1997), while MSCs are highly resistant to oxidative stress (Elshemy et al., 2021). MSCs derived from different sources have an anti-apoptotic ability that reduces ROS levels and contributes to repairing damaged tissues. Notably, MSC transplantation upregulated antioxidant enzymes, reduced kidney injury (Li et al., 2012), and enhanced cardiac regenerative capability (Chen et al., 2021) in diabetic animal models. Here, we explored the molecular mechanisms by which hUC-MSCs reduce oxidative stress and improve pancreatic β-cell function under hyperglycaemic conditions. Nrf2 induces a large number of detoxification and antioxidant enzymes, which have strong protective capacities against various environmental stresses. Nrf2 activation protects islet β-cells from ROS induced by acute high-glucose stimulation (Schultheis et al., 2019). Genetic activation of the Nrf2 signalling pathway significantly suppressed the onset of diabetes (Uruno et al., 2013). While Nrf2 depletion contributes to worsening glucose tolerance in adipose tissue and the liver (Beyer et al., 2008; Xue et al., 2013), it also increases renal oxidative stress and accelerates chronic kidney injury in STZ-induced diabetic mice (Yoh et al., 2008). Consistent with previous studies, our data showed that hUC-MSC treatment upregulated Nrf2 expression and had a beneficial effect on pancreatic β-cell function under high-glucose conditions. Furthermore, Nrf2 knockdown impaired the therapeutic effects, suggesting that hUC-MSCs might repair oxidative stress-induced pancreatic β-cell injury by regulating the Nrf2/HO-1 pathway. To date, several

Figure 7 *(Continued)* (**D**) Intracellular ROS were assessed by flow cytometry. (**E**) GSIS in INS-1E cells was measured at 1 h after glucose stimulation (16.7 mM) by ELISA. (**F** and **G**) Protein levels of Nrf2, HO-1 (**F**), PDX-1, GLUT2, MafA, BCL-2, and cleaved Caspase-3 (**G**) in INS-1E cells were measured by western blotting. Protein expression levels were normalized to GAPDH. Data are presented as mean ± SEM. $^{*}P < 0.05$, $^{**}P < 0.01$.

pharmacological activators of the Nrf2/HO-1 signalling pathway have been explored for treating diabetic complications due to their antioxidant properties. For example, hydrogen sulphide could reduce aortic atherosclerotic plaque formation and suppress the development of diabetes-accelerated atherosclerosis, which is attributed to anti-oxidative effects via the Nrf2 signalling pathway (Xie et al., 2016). Furthermore, phosphocreatine protects kidney cells from oxidative stress and apoptosis caused by diabetes through activating the Nrf2/HO-1 pathway (Shopit et al., 2020). Our findings demonstrate, for the first time, that the Nrf2/HO-1 signalling pathway activated by hUC-MSC treatment attenuates oxidative stress-induced ROS overproduction, cell apoptosis, and insulin secretion defects in STZ-induced diabetic mice.

In summary, we systematically evaluated the protective effects of hUC-MSCs on high glucose-stimulated islet β-cells and showed that hUC-MSCs can improve β-cell function under high-glucose conditions and inhibit oxidative stress and ROS production by activating Nrf2 signalling (Figure 8). Therefore, hUC-MSC transplantation may provide new insights into diabetes treatment, and the Nrf2/HO-1 defence system may also be a novel target.

Materials and methods

Isolation and identification of hUC-MSCs

hUC-MSCs were obtained from the Translational Medical Center for Stem Cell Therapy of Shanghai East Hospital. The Ethics Committee of Shanghai East Hospital approved the experimental protocol. Clinical-grade MSCs were then generated under good manufacturing practice conditions, as accredited by Shanghai East Hospital. Briefly, the umbilical cord was cut into small tissue pieces after removing the umbilical artery and vein. Tissue pieces were cultivated in MEM α (Gibco) supplemented with 10% UltraGROTM (AventaCell) at 37°C in a 5% CO_2 atmosphere. After 1 week, the cells migrated and visibly adhered to the dish surface. Then, the cells were digested for subculture. Cells cultured to passage 4 were used in experiments after sterility testing, mycoplasma detection, and characterization of surface markers (CD73/CD90/CD105/CD11/CD31/CD34/CD45/HLA-DR).

To evaluate the multi-lineage differentiation potential, hUC-MSCs were incubated in adipogenic, osteogenic, and chondrogenic differentiation media (Cyagen) for 3 weeks. For adipogenesis, the cell pellets were stained with oil red O to detect the intracellular accumulation of lipid vacuoles. Bone matrix formation, as measured by alizarin red S staining, demonstrated osteogenesis. Chondrogenesis was confirmed by the secretion of sulphated glycosaminoglycans stained with alcian blue.

DM animal model and hUC-MSC administration

All animal procedures were approved by the Animal Care and Experimental Committee of Shanghai Sixth People's Hospital Affiliated to Shanghai Jiao Tong University School of Medicine. Eight-week-old male C57BL/6J mice (20–23 g) were purchased from Shanghai SLAC Laboratory Animal Corporation. The mice were maintained on a 12-h:12-h light–dark cycle and fed normal chow. For the diabetic model, mice were injected intraperitoneally with a single dose of 100 mg/kg STZ (Sigma-Aldrich) after overnight fasting. STZ was solubilized in sodium citrate buffer (pH 4.5) and injected within 30 min of preparation. Random glucose level was consecutively measured by monitoring tail capillary blood glucose levels every 3 days during the experiments. Blood glucose levels were determined using a glucose metre (ACCU-CHEK, Roche). Mice with at least three times of random blood glucose level $\geq$16.7 mmol/L were defined as diabetic mice. IPGTTs were conducted to confirm the established diabetic model (Supplementary Figure S1). For IPGTTs, mice were fasted overnight and intraperitoneally injected with glucose (2.0 g/kg). Glucose levels were determined using tail blood samples taken at 0, 15, 30, 60, and 120 min after the injection. The diabetic mice were randomly divided into two groups: DM and DM+hUC-MSCs ($n = 6$ each group). The DM+hUC-MSCs group was administered with an infusion of 1×10^6 hUC-MSCs (at passage 4) suspended in 0.2 ml PBS via the tail vein every 7 days. The DM group was treated with 0.2 ml PBS alone. Mice without STZ injection were used as normal controls. To evaluate the therapeutic effects of hUC-MSCs, IPGTTs were also performed on mice before sacrifice. Glucose (2.0 g/kg) was intraperitoneally injected into 6-h-fasted mice. Blood samples were collected from the tail vein. The amount of serum insulin was determined using the mouse insulin ELISA (CrystalChem) following the manufacturer's instructions.

Histological analysis

Mouse pancreases were excised and fixed in 4% formalin for 24 h at 4°C. Fixed tissues were processed for paraffin embedding, and serial 4-μm-thick sections were prepared. For immunofluorescence staining, slides were deparaffinized and rehydrated, and antigen retrieval was performed using antigen unmasking buffer; the slides were then blocked for 60 min at room temperature in 5% bovine serum albumin (BSA) and PBS. To determine islet endocrine composition, the sections of paraffin-embedded pancreas were incubated overnight with primary antibodies against insulin (Guinea pig, Dako), glucagon (1:2000, mouse, Abcam), PDX-1 (1:300, rabbit, Cell Signaling Technology), and GLUT2 (1:1000, rabbit, Proteintech) at 4°C, after which the sections were incubated in the secondary antibody with rhodamine (1:500) at 37°C for 30 min. The nuclear regions were stained with DAPI. The slides were digitized using a Pannoramic MIDI scanner (3DHISTECH), and the images were captured using CaseViewer slide management software (3DHistech). The images were further analysed using ImageJ version 1.49v software.

In vivo imaging of fluorescently labelled hUC-MSCs

To study hUC-MSC bio-distribution in diabetic mice, a near-infrared fluorescence dye, DiR (D12731, Invitrogen), was used

to label cells. Briefly, cells were incubated with a suspension of DiR at 37°C for 30 min. Afterwards, the cells were washed with PBS twice and suspended for cell transplantation. Then, 1×10^6 DiR-labelled hUC-MSCs suspended in 0.2 ml PBS were intravenously injected into diabetic mice. The control group was treated with the same volume of PBS. At 1, 3, and 7 days after cell infusion, *in vivo* imaging and *ex vivo* imaging were carried out using IVIS® Spectrum Imaging System (PerkinElmer) to monitor DiR-labelled hUC-MSCs and their tissue distribution. The mice were anesthetized before *in vivo* imaging. *Ex vivo* fluorescence detection of all organs (liver, lung, spleen, pancreas, kidney, and heart) was performed immediately after the animals were sacrificed.

Cells and cell culture

INS-1E cells were kindly provided by the Shanghai Key Laboratory of Diabetes Mellitus. The cells were cultured in complete RPMI-1640 medium (Gibco) with 11.1 mM glucose. The medium was supplemented with 1% streptomycin/penicillin (Gibco), 10% foetal bovine serum (Gibco), 1 mM sodium pyruvate, 10 mM HEPES, and 0.05 mM β-mercaptoethanol. The medium was replaced every 2 days until INS-1E cells reached a confluency of 80%–90%.

Co-culture of INS-1E cells and hUC-MSCs

A co-culture system was established using Transwell inserts with a pore size of 0.4 μm (Corning). INS-1E cells were pre-seeded in the bottom well in complete medium 24 h before co-culture to allow cells to adhere. hUC-MSCs (5×10^4) were seeded into the upper inserts. Thereafter, INS-1E cells were cultured with or without hUC-MSCs and incubated in complete RPMI-1640 medium for 24 h. Glucotoxicity was induced by applying 30 mM glucose in complete RPMI-1640 medium. Cells incubated in normal medium served as the background control. At the end of the experiment, the upper inserts were removed, and INS-1E cells were washed with PBS for further analysis.

GSIS test

GSIS test was performed to assess the insulin secretion capacity of cells. INS-1E cells were pre-treated with Krebs–Ringer bicarbonate HEPES (KRBH, supplemented with 1% BSA) buffer without glucose for 1 h. Then, cells were incubated with KRBH buffer containing 2.8 mM glucose for 1 h, followed by incubation with KRBH buffer containing 16.7 mM glucose for another 1 h. The amount of insulin in the medium was determined using the rat insulin ELISA (CrystalChem) following the manufacturer's instructions. Secreted insulin was normalized to total protein levels.

Cell proliferation assay

A Cell Counting Kit-8 (CCK-8) assay was performed to evaluate cell proliferation. INS-1E cells ($\sim 2 \times 10^4$ cells/well) were seeded into a 96-well plate, and the total volume was made up to 100 μl with RPMI-1640 medium. CCK-8 solution (10 μl) was added at 0, 24, 48, and 72 h of culture, respectively, followed by 1 h of incubation. Finally, the optical density value was measured using an ELISA plate reader at 450 nm.

Cell apoptosis by flow cytometry

INS-1E cell apoptosis was detected with an Annexin V-FITC/PI Apoptosis Detection Kit (Yeasen). The cells were harvested, stained with FITC-conjugated Annexin V and PI for 15 min at room temperature in the dark, and detected using flow cytometry (Beckman Coulter).

ROS measurement

A DCFH-DA probe was used to measure intracellular ROS. Briefly, cells were washed with PBS before adding the DCFH-DA probe (10 μM), followed by incubation at 37°C for 30 min in the dark. The cells were then washed with PBS and re-suspended in RPMI-1640 medium. The intracellular ROS level was evaluated using flow cytometry (Beckman Coulter).

Transfection of hUC-MSCs with Nrf2 siRNA

INS-1E cells were transfected with 20 nM Nrf2 siRNA (5′-GGATGAAGAGACCGGAGAA-3′) or a negative control (Shanghai Asia-Vector Biotechnology) using Lipo3000 reagent (Invitrogen) following the manufacturer's instructions. To confirm Nrf2 knockdown, protein and RNA were extracted from INS-1E cells and assayed by western blotting and quantitative real-time polymerase chain reaction (PCR), respectively. The following primers were used: *Nrf2* forward primer: TTGGCAGAGACATTCCCATTTGTA, reverse primer: GAGCTATCGAGTGACTGAGCCTGA; *Ho-1* forward primer: CAGGGTGACAGAAGAGGCTAAG, reverse primer: CTGTGAGGGACTCTGGTCTTTG. INS-1E cells were transfected for 48 h before the medium was replaced with co-culture medium. Next, hUC-MSCs were placed in or within the upper inserts for another 24 h for co-culture experiments. Thereafter, the upper inserts were removed, and the INS-1E cells were washed with PBS for further analysis.

ELISA

Mouse fasting blood samples were collected from the tail vein, and serum was obtained by centrifugation at 12000 rpm for 5 min. The fasting serum samples were stored at −80°C until they were used for assays. The insulin concentration of the mouse serum or cell culture medium was examined using ELISA kits (CrystalChem) following the manufacturer's instructions.

Western blotting

Cell and pancreatic tissue lysates were prepared in ice-cold cell lysis buffer (Beyotime Institute of Biotechnology) containing a cocktail of proteinase inhibitors (MedChemExpress) and centrifuged at 14000 rpm for 30 min at 4°C. Next, the extracted total protein (30 μg) was electrophoresed on a 10% SDS–PAGE gel and transferred to PVDF membranes (Millipore). The membranes were then blocked with 5% non-fat milk for 1 h. Subsequently, the membranes were incubated with the indicated primary

antibodies against GLUT2 (1:1000, Proteintech, #20436), MafA (1:1000, Abcam, ab26405), PDX-1 (1:1000, Proteintech, #20989), BCL-2 (1:1000, Proteintech, #60718), cleaved Caspase-3 (1:1000, Cell Signaling Technology, #9661S), Nrf2 (1:1000, Abcam, ab137550; 1:1000, Cell Signaling Technology, #33649S), HO-1 (1:1000, Cell Signaling Technology, #82206), β-actin (1:20000, Abcam, ab8226), and GAPDH (1:20000, Cell Signaling Technology, #5174) overnight at 4°C and then incubated with HRP-conjugated secondary antibodies for 60 min at room temperature. Finally, the protein bands were detected using an ECL system.

Quantitative real-time PCR

Total RNA was extracted from INS-1E cells using TRIzol reagent (Invitrogen) and reverse-transcribed into cDNA with a reverse transcription kit (Vazyme) following the manufacturer's instructions. Real-time PCR analysis was performed using SYBR Green Real-time PCR Reagent (Vazyme) via an ABI Prism 7300 Thermal Cycler (Applied Biosystems). The results were normalized to the 18S gene. The relative mRNA expression levels were calculated using the formula $2^{-\Delta\Delta Ct}$.

Statistical analysis

Statistical analysis was performed using GraphPad Prism 8.0 software. Statistical differences were analysed via two-tailed Student's *t*-test. $P < 0.05$ was considered statistically significant. All data are presented as mean ± standard error of the mean (SEM).

Supplementary material

Supplementary material is available at *Journal of Molecular Cell Biology* online.

Acknowledgements

We would like to thank Wenwen Jia (Shanghai East Hospital, Tongji University) for kindly providing hUC-MSCs. We also thank Yinan Zhang (Shanghai Sixth People's Hospital Affiliated to Shanghai Jiao Tong University School of Medicine) for his useful discussion and Yi Eve Sun (Tongji Hospital, Tongji University) for technical assistance.

Funding

This study was supported by grants from the National Natural Science Foundation of China (82070913), Shanghai Science and Technology Development Funds (20ZR1446000 and 22410713200), the Research Start-up Fund from Shanghai Fourth People's Hospital (sykyqd01801), and the Open Research Project of Shanghai Key Laboratory of Diabetes Mellitus (SHKLD-KF-2101).

Conflict of interest: none declared.

Author contributions: P.L. and C.W. designed the experiments; P.L. performed the experiments and acquired the data; P.L., B.C., and C.W. drafted and revised the manuscript. All the authors approved the submission of this paper.

References

Aguayo-Mazzucato, C., and Bonner-Weir, S. (2010). Stem cell therapy for type 1 diabetes mellitus. Nat. Rev. Endocrinol. *6*, 139–148.

Alunno, A., Montanucci, P., Bistoni, O., et al. (2015). In vitro immunomodulatory effects of microencapsulated umbilical cord Wharton jelly-derived mesenchymal stem cells in primary Sjogren's syndrome. Rheumatology *54*, 163–168.

Beyer, T.A., Xu, W., Teupser, D., et al. (2008). Impaired liver regeneration in Nrf2 knockout mice: role of ROS-mediated insulin/IGF-1 resistance. EMBO J. *27*, 212–223.

Cai, J., Wu, Z., Xu, X., et al. (2016). Umbilical cord mesenchymal stromal cell with autologous bone marrow cell transplantation in established type 1 diabetes: a pilot randomized controlled open-label clinical study to assess safety and impact on insulin secretion. Diabetes Care *39*, 149–157.

Cao, H., Cheng, Y., Gao, H., et al. (2020). In vivo tracking of mesenchymal stem cell-derived extracellular vesicles improving mitochondrial function in renal ischemia–reperfusion injury. ACS Nano *14*, 4014–4026.

Carlsson, P.-O., Schwarcz, E., Korsgren, O., et al. (2015). Preserved β-cell function in type 1 diabetes by mesenchymal stromal cells. Diabetes *64*, 587–592.

Chen, T.-S., Chuang, S.-Y., Shen, C.-Y., et al. (2021). Antioxidant Sirt1/Akt axis expression in resveratrol pretreated adipose-derived stem cells increases regenerative capability in a rat model with cardiomyopathy induced by diabetes mellitus. J. Cell. Physiol. *236*, 4290–4302.

Chen, X., Liang, H., Xi, Z., et al. (2020). BM-MSC transplantation alleviates intracerebral hemorrhage-induced brain injury, promotes astrocytes vimentin expression, and enhances astrocytes antioxidation via the Cx43/Nrf2/HO-1 axis. Front. Cell Dev. Biol. *8*, 302.

Chrostek, M.R., Fellows, E.G., Crane, A.T., et al. (2019). Efficacy of stem cell-based therapies for stroke. Brain Res. *1722*, 146362.

Elshemy, M.M., Asem, M., Allemailem, K.S., et al. (2021). Antioxidative capacity of liver- and adipose-derived mesenchymal stem cell-conditioned media and their applicability in treatment of type 2 diabetic rats. Oxid. Med. Cell. Longev. *2021*, 8833467.

Gao, X., Song, L., Shen, K., et al. (2014). Bone marrow mesenchymal stem cells promote the repair of islets from diabetic mice through paracrine actions. Mol. Cell. Endocrinol. *388*, 41–50.

Hu, J., Yu, X., Wang, Z., et al. (2013). Long term effects of the implantation of Wharton's jelly-derived mesenchymal stem cells from the umbilical cord for newly-onset type 1 diabetes mellitus. Endocr. J. *60*, 347–57.

Katsarou, A., Gudbjörnsdottir, S., Rawshani, A., et al. (2017). Type 1 diabetes mellitus. Nat. Rev. Dis. Primers *3*, 17016.

Kim, W.-H., Lee, J.W., Suh, Y.H., et al. (2007). AICAR potentiates ROS production induced by chronic high glucose: roles of AMPK in pancreatic β-cell apoptosis. Cell. Signal. *19*, 791–805.

Kono, T.M., Sims, E.K., Moss, D.R., et al. (2014). Human adipose-derived stromal/stem cells protect against STZ-induced hyperglycemia: analysis of hASC-derived paracrine effectors. Stem Cells *32*, 1831–1842.

Li, M., Vanella, L., Zhang, Y., et al. (2012). Stem cell transplantation increases antioxidant effects in diabetic mice. Int. J. Biol. Sci. *8*, 1335–1344.

Liu, W., Wang, Y., Gong, F., et al. (2019). Exosomes derived from bone mesenchymal stem cells repair traumatic spinal cord injury by suppressing the activation of A1 neurotoxic reactive astrocytes. J. Neurotrauma *36*, 469–484.

Lu, T.-H., Su, C.-C., Chen, Y.-W., et al. (2011). Arsenic induces pancreatic β-cell apoptosis via the oxidative stress-regulated mitochondria-dependent and endoplasmic reticulum stress-triggered signaling pathways. Toxicol. Lett. *201*, 15–26.

Lv, W., Graves, D.T., He, L., et al. (2020). Depletion of the diabetic gut microbiota resistance enhances stem cells therapy in type 1 diabetes mellitus. Theranostics *10*, 6500–6516.

Ma, Y., Wang, L., Yang, S., et al. (2021). The tissue origin of human mesenchymal stem cells dictates their therapeutic efficacy on glucose and lipid metabolic disorders in type II diabetic mice. Stem Cell Res. Ther. *12*, 385.

Maldonado, M., Huang, T., Yang, L., et al. (2017). Human umbilical cord Wharton jelly cells promote extra-pancreatic insulin formation and repair of renal damage in STZ-induced diabetic mice. Cell Commun. Signal. *15*, 43.

Matés, J.M. (2000). Effects of antioxidant enzymes in the molecular control of reactive oxygen species toxicology. Toxicology *153*, 83–104.

Meier, J.J., Bhushan, A., Butler, A.E., et al. (2005). Sustained β cell apoptosis in patients with long-standing type 1 diabetes: indirect evidence for islet regeneration? Diabetologia *48*, 2221–2228.

Motegi, S.-I., Sekiguchi, A., Uchiyama, A., et al. (2017). Protective effect of mesenchymal stem cells on the pressure ulcer formation by the regulation of oxidative and endoplasmic reticulum stress. Sci. Rep. *7*, 17186.

Pellegrini, S., Piemonti, L., and Sordi, V. (2018). Pluripotent stem cell replacement approaches to treat type 1 diabetes. Curr. Opin. Pharmacol. *43*, 20–26.

Rahavi, H., Hashemi, S.M., Soleimani, M., et al. (2015). Adipose tissue-derived mesenchymal stem cells exert in vitro immunomodulatory and beta cell protective functions in streptozotocin-induced diabetic mice model. J. Diabetes Res. *2015*, 878535.

Schultheis, J., Beckmann, D., Mulac, D., et al. (2019). Nrf2 activation protects mouse β cells from glucolipotoxicity by restoring mitochondrial function and physiological redox balance. Oxid. Med. Cell. Longev. *2019*, 7518510.

Shalaby, S.M., El-Shal, A.S., Abd-Allah, S.H., et al. (2014). Mesenchymal stromal cell injection protects against oxidative stress in Escherichia coli-induced acute lung injury in mice. Cytotherapy *16*, 764–775.

Shaw, P., and Chattopadhyay, A. (2020). Nrf2–ARE signaling in cellular protection: mechanism of action and the regulatory mechanisms. J. Cell. Physiol. *235*, 3119–3130.

Shopit, A., Niu, M., Wang, H., et al. (2020). Protection of diabetes-induced kidney injury by phosphocreatine via the regulation of ERK/Nrf2/HO-1 signaling pathway. Life Sci. *242*, 117248.

Tiedge, M., Lortz, S., Drinkgern, J., et al. (1997). Relation between antioxidant enzyme gene expression and antioxidative defense status of insulin-producing cells. Diabetes *46*, 1733–1742.

Ullah, M., Liu, D.D., and Thakor, A.S. (2019). Mesenchymal stromal cell homing: mechanisms and strategies for improvement. iScience *15*, 421–438.

Uruno, A., Furusawa, Y., Yagishita, Y., et al. (2013). The Keap1–Nrf2 system prevents onset of diabetes mellitus. Mol. Cell. Biol. *33*, 2996–3010.

Uruno, A., Yagishita, Y., and Yamamoto, M. (2015). The Keap1–Nrf2 system and diabetes mellitus. Arch. Biochem. Biophys. *566*, 76–84.

Wang, L., Qing, L., Liu, H., et al. (2017). Mesenchymal stromal cells ameliorate oxidative stress-induced islet endothelium apoptosis and functional impairment via Wnt4–β-catenin signaling. Stem Cell Res. Ther. *8*, 188.

Xie, L., Gu, Y., Wen, M., et al. (2016). Hydrogen sulfide induces Keap1 S-sulfhydration and suppresses diabetes-accelerated atherosclerosis via Nrf2 activation. Diabetes *65*, 3171–3184.

Xue, P., Hou, Y., Chen, Y., et al. (2013). Adipose deficiency of Nrf2 in ob/ob mice results in severe metabolic syndrome. Diabetes *62*, 845–854.

Yaochite, J.N., de Lima, K.W., Caliari-Oliveira, C., et al. (2016). Multipotent mesenchymal stromal cells from patients with newly diagnosed type 1 diabetes mellitus exhibit preserved in vitro and in vivo immunomodulatory properties. Stem Cell Res. Ther. *7*, 14.

Yin, Y., Hao, H., Cheng, Y., et al. (2018). The homing of human umbilical cord-derived mesenchymal stem cells and the subsequent modulation of macrophage polarization in type 2 diabetic mice. Int. Immunopharmacol. *60*, 235–245.

Yoh, K., Hirayama, A., Ishizaki, K., et al. (2008). Hyperglycemia induces oxidative and nitrosative stress and increases renal functional impairment in Nrf2-deficient mice. Genes Cells *13*, 1159–1170.

Zhang, G., Zou, X., Huang, Y., et al. (2016). Mesenchymal stromal cell-derived extracellular vesicles protect against acute kidney injury through anti-oxidation by enhancing Nrf2/ARE activation in rats. Kidney Blood Press. Res. *41*, 119–128.

Zhang, P., Li, T., Wu, X., et al. (2020). Oxidative stress and diabetes: antioxidative strategies. Front. Med. *14*, 583–600.

Zhao, K., Hao, H., Liu, J., et al. (2015). Bone marrow-derived mesenchymal stem cells ameliorate chronic high glucose-induced β-cell injury through modulation of autophagy. Cell Death Dis. *6*, e1885.

Zhou, Y., Hu, Q., Chen, F., et al. (2015). Human umbilical cord matrix-derived stem cells exert trophic effects on β-cell survival in diabetic rats and isolated islets. Dis. Model. Mech. *8*, 1625–1633.

Received May 11, 2022. Revised January 10, 2023. Accepted February 14, 2023.